Constraints on dissipative unified dark matter

Hermano Velten[a,b] **and Dominik J. Schwarz**[b]

[a]Universidade Federal do Espírito Santo, Av. Fernando Ferrari, Goiabeiras, Vitória, Brasil
[b]Fakultät für Physik, Universität Bielefeld, Postfach 100131, 33501 Bielefeld, Germany

E-mail: velten@physik.uni-bielefeld.de, dschwarz@physik.uni-bielefeld.de

Abstract. Modern cosmology suggests that the Universe contains two dark components – dark matter and dark energy – both unkown in laboratory physics and both lacking direct evidence. Alternatively, a unified dark sector, described by a single fluid, has been proposed. Dissipation is a common phenomenon in nature and it thus seems natural to consider models dominated by a viscous dark fluid. We focus on the study of bulk viscosity, as isotropy and homogeneity at large scales implies the suppression of shear viscosity, heat flow and diffusion. The generic ansatz $\xi \propto \rho^\nu$ for the coefficient of bulk viscosity (ρ denotes the mass/energy density), which for $\nu = -1/2$ mimics the ΛCDM background evolution, offers excellent fits to supernova and H(z) data. We show that viscous dark fluids suffer from large contributions to the integrated Sachs-Wolfe effect (generalising a previous study by Li & Barrow) and a suppression of structure growth at small-scales (as seen from a generalized Meszaros equation). Based on recent observations, we conclude that viscous dark fluid models (with $\xi \propto \rho^\nu$ and neglecting baryons) are strongly challenged.

Contents

1   Introduction

The cosmological concordance model states that the Universe is spatially flat and approximately 95% of its energy content is made up of an unknown dark sector. The remaining 5% is known: baryonic matter, electrons, photons and neutrinos. In the context of the concordance model a quarter of the dark sector behaves like cold dark matter (CDM), a pressureless component that clusters. The remaining dark stuff is called dark energy and is hold responsable for the current accelerated expansion of the Universe.

Dark energy is commonly modeled either by a scalar field or a dissipationless fluid. The isotropy and homogeneity of the Universe at large scales, suggests that such a fluid description makes sense, at least as an effective description. Then dark energy has negative pressure, such that its equation of state $p \sim -\rho$ today. Alternatively, one might view dark matter and dark energy as different manifestations of one single substance – unified dark matter. Its equation of state function $w \equiv p/\rho$ must be time-dependent in order to interpolates from the matter dominated epoch to the current accelerated expansion.

In this work we study a single-fluid descriptions of the dark sector. As long as only the homogeneous and isotropic evolution (the background) is concerned, this class of models is indistinguishable from the concordance model. However, when it comes to perturbations differences become apparent at late times. We investigate in detail their contributions to the integrated Sachs-Wolfe effect, which probes most efficiently the large scales at late times, and the small-scale matter power spectrum, which probes the other side of the structure formation. We demonstrate that a generic single-fluid description of the Universe seems to be strongly challenged from both sides.

A prominent candidate for this scenario is the Chaplygin gas, where $p_{\rm c} = -A/\rho_{\rm c}$, and its generalized version $p_{\rm gc} = -A/\rho_{\rm gc}^{\alpha}$ [1]. For the case $\alpha = 1$, this exotic equation of state is motivated by string theory, where the Chaplygin gas is interpreted as an effective description

of a gas of D-branes in a D+2-dimensional space-time [2]. For the background evolution, $\alpha = 0$ corresponds to the Λ cold dark matter model (ΛCDM).

Another popular candidate is a dissipative fluid with intrinsic bulk viscosity [3, 4]. Any real fluid shows dissipative phenomena and thus it is well motivated to include this aspect in cosmology as well. Typically shear viscosity is more important than bulk viscosity, however isotropy and homogeneity of the Universe at large scales, does not allow for shear. From the same argument diffusion and heat conduction cannot play an important role. Thus at large scales, bulk viscosity must be the dominant dissipative effect. For an expanding universe it gives rise to a negative contribution to pressure, $p_{\rm v} = -\xi\Theta$, where Θ is the volume expansion rate of the fluid and $\xi > 0$ is the coefficient of bulk viscosity. In order to study the cosmic expansion, one needs to specify $\xi = \xi(t)$. A common ansatz, which we will adopt below, is $\xi \propto \rho^{\nu}$ [5].

The generalized Chaplygin gas (GCG) and the viscous dark fluid (VDF) have the same background dynamics in the one-fluid approximation [10]. However, the difference between these fluids appears at perturbative level. While the GCG is viewed as a dissipationless fluid, it has isentropic (the same entropy everywhere) perturbations $\delta p_{\rm gc} = (\dot{p}_{\rm gc}/\dot{\rho}_{\rm gc})\delta\rho_{\rm gc}$, the perturbative dynamics of the VDF is, by definition, nonadiabatic and it could also be non-isentropic, $\delta p_{\rm v} \neq (\dot{p}_{\rm v}/\dot{\rho}_{\rm v})\delta\rho_{\rm v}$.

As GCG and VDF are equivalent w.r.t. their background evolution, both models can fit probes that are not sensitive to structure formation itself, e.g. SNIa data [6]. At the perturbative level one obtains, from the matter power spectrum and from the cosmic microwave background (CMB) spectrum, very different predictions. The confrontation of the GCG model with the matter power spectrum data, provided by the Sloan Digital Sky Survey (SDSS) and the Two Degree Field Galaxy Redshift Survey (2dFGRS) data sets, discards a one-fluid GCG universe [7] due to strong oscillations in its theoretical power spectrum. However, it has been demonstrated that this problem is solved when a baryonic component is taken into account [8] or, if *ad hoc* entropy perturbations are included in the GCG perturbative dynamics [9]. While the former is a trivial solution, as the observed power spectrum corresponds to the visible matter and not the dark one, the latter can be seen as a motivation to explore viscous (intrinsically nonadiabatic) cosmologies. On the other hand, the bulk viscous model does not show the same pathologies as the GCG, thanks to its nonadiabatic behavior [10, 11]. The GCG with $\alpha \approx 0$ agrees with CMB data [12], while, apparently, the VDF does not, due to a huge amplification of the integrated Sachs-Wolfe (ISW) signal [13].

The authors of [13] showed that, the evolution of the gravitational potential in a VDF model differs from the ΛCDM model at late times, implying a huge ISW effect. This is also found for the GCG [12] and for general unified dark matter cosmologies relying on a single scalar field [14]. However, these studies have been limited to fixed values of the cosmological parameters and it remains unclear, if the huge ISW effect could be avoided in a different region of parameter space. We study the dependence of the ISW effect on the model parameters of VDF models and GCG models.

We also study the behaviour of sub horizon pertubations in the VDF and GCG models during the matter dominated epoch. We show that structure formation can be drastically affected in such cosmologies by comparing the growth of the unified dark matter perturbations with a typical CDM scenario. In other words, we investigate whether dark halos, the hosts of galaxies can form at all.

In the next section, we compare the background evolution of the GCG and VDF models with ΛCDM. Section 3 is devoted to the study of linear perturbations. We provide an

evolution equation for the study of the ISW effect and we obtain Meszaros-like equations for the evolution of sub-horizon perturbations in the VDF and GCG models. In section 4 we derive quantitative results for unified dark matter cosmologies and conclude with some remarks and open issues in the final section.

2 Background evolution

In this work, we assume a spatially flat one-fluid description of the matter content of the Universe. This ansatz is expected to be appropriate at late times (thus radiation is negligible). At small scales we also neglect the effects of baryonic matter, which limits the precision of our discussion to the 10% to 20% level at small scales.

The description of relativistic viscous fluids allows for a freedom in the choice of the comoving frame. Comoving observers could be comoving with energy transport (Landau-frame) or with particle number transport (Eckart-frame). Both approaches are equivalent, but one has to make a choice. Here we adopt the Eckart formalism [15]. Then, the VDF bulk pressure is given by $p_{\rm v} = -\xi\Theta$. Due to the second law of thermodynamics the coefficient of bulk viscosity $\xi \geq 0$. The volume expansion rate $\Theta \equiv u^{\mu}_{;\mu}$ (Greek indices run from 0 to 3, ";" denotes a covariant derivative) is obtained from the fluid velocity u^{μ}. In a homogeneous and isotropic Universe, $\Theta = 3H$, where H is the Hubble expansion rate. With the ansatz

$$\xi = \xi_0 \left(\frac{\rho}{\rho_0} \right)^{\nu}, \tag{2.1}$$

and assuming that the kinetic pressure $p = 0$, the bulk viscous pressure of the background becomes [by means of $H = H_0(\rho/\rho_0)^{1/2}$]

$$p_{\rm v} = -3H_0\xi_0 \left(\frac{\rho}{\rho_0} \right)^{\nu+1/2}. \tag{2.2}$$

The GCG model has a similar equation of state, $p_{\rm gc} = -A\rho_0 \left(\rho_0/\rho\right)^{\alpha}$, with A and α being dimensionless parameters.

In a perfectly homogeneous and isotropic Universe, the GCG model and the VDF are equivalent, which is easily verified by the replacements $\alpha = -(\nu + \frac{1}{2})$ and $A = 3H_0\xi_0/\rho_0$. Hence, both fluids show the same time evolution. Instead of ξ_0 or A, it also is convenient to use the deceleration parameter q_0. This correspondence can be established by

$$q_0 = \frac{1}{2}(1 - 3A) = \frac{1}{2} \left(1 - \frac{9H_0\xi_0}{\rho_0} \right). \tag{2.3}$$

Once $\xi_0 > 0$, then $q_0 < 1/2$. The background evolution of the VDF and the GCG is governed by (a denotes the scale factor and $a_0 = 1$)

$$\left(\frac{H_{\rm v}}{H_0} \right)^2 = \left[\frac{3H_0\xi_0}{\rho_0} + \frac{1 - \frac{3H_0\xi_0}{\rho_0}}{a^{3(\frac{1}{2}-\nu)}} \right]^{\frac{1}{\frac{1}{2}-\nu}} \tag{2.4}$$

and

$$\left(\frac{H_{\rm gc}}{H_0} \right)^2 = \left[A + \frac{1 - A}{a^{3(1+\alpha)}} \right]^{\frac{1}{1+\alpha}}, \tag{2.5}$$

respectively. The existence of an early matter dominated epoch, $H(a \ll 1) \sim a^{-3/2}$, is guaranteed for $\nu < 1/2$ and $\xi_0 < \rho_0/(3H_0)$ for the VDF model and for $\alpha > -1$ and $A < 1$ in the GCG case. In order to obtain an accelerated epoch at late times ($q_0 < 0$), the parameters must obey $\xi_0 > \rho_0/(9H_0)$ and $A > 1/3$, respectively. The early and late time limits of both models are equivalent to the ΛCDM model. The only difference is the transition from the matter dominated phase to the accelerated epoch, which is given by the equation of state functions

$$w_{\mathrm{v}} \equiv \frac{-3H\xi}{\rho} = \frac{-1}{1 + \frac{\rho_0 - 3H_0\xi_0}{3H_0\xi_0}(1+z)^{3(\frac{1}{2}-\nu)}} \tag{2.6}$$

and

$$w_{\mathrm{gc}} = \frac{p_{\mathrm{gc}}}{\rho} = \frac{-1}{1 + \frac{(1-A)}{A}(1+z)^{3(1+\alpha)}}. \tag{2.7}$$

The expressions in (2.5) are analogue to the ΛCDM one,

$$\left(\frac{H_\Lambda}{H_0}\right)^2 = \frac{\Omega_{m0}}{a^3} + 1 - \Omega_{m0}, \tag{2.8}$$

if we adopt $q_0 = \frac{3\Omega_{m0}}{2} - 1$ ($A = 1 - \Omega_{m0}$) and $\nu = -1/2$ ($\alpha = 0$) for the VDF (GCG) model. These relations will be usefull in the next section in order to compare the perturbative dynamics of these models.

3   Density perturbations of a dissipative fluid

In this section we study the perturbative dynamics for the VDF and the GCG models. The differences between both models for an inhomogeneous Universe can be traced back to an inherent nonadiabatic behavior of the viscous model. In a sense, the VDF model can be seen as a nonadiabatic version of the GCG model.

Let us start by considering the most general dissipative fluid with energy momentum tensor T_ν^μ, including a dissipative contribution which is denoted by ΔT_ν^μ. In the Eckart frame, the most general dissipative tensor is

$$\Delta T_\nu^\mu = -\xi \Delta T_{b\ \nu}^\mu - \eta \Delta T_{s\ \nu}^\mu - \kappa \Delta T_{h\ \nu}^\mu, \tag{3.1}$$

where ξ, η and κ are the coefficients of bulk viscosity, shear viscosity and heat conduction. For the homogeneous and isotropic background, only the bulk viscosity contributes to the cosmic dynamics. At first order, the heat conduction contributes only to the non-diagonal elements of ΔT_ν^μ, and thus producing negligible contributions on superhorizon scales. The same happens with shear viscosity. In contrast to bulk viscosity, shear viscosity and heat conduction, influence the evolution of cosmological perturbations via spatial gradients.

In the following we neglect heat conduction and shear viscosity also at the level of perturbations and thus the cosmic fluid is described by the energy-momentum tensor

$$T_\nu^\mu = \rho u^\mu u_\nu + p h_\nu^\mu + \Delta T_\nu^\mu = \rho u^\mu u_\nu + p h_\nu^\mu - \xi u_{;\gamma}^\gamma h_\nu^\mu, \tag{3.2}$$

where $h^{\mu\nu} = g^{\mu\nu} + u^\mu u^\nu$. More explicity, the background components of (3.2) are

$$T_0^0 = -\rho, \quad T_i^0 = T_0^i = 0, \quad T_j^i = p_{\mathrm{eff}}\delta_j^i = \left(p - \frac{3\xi\mathcal{H}}{a}\right)\delta_j^i, \tag{3.3}$$

where $\mathcal{H} = \frac{a'}{a}$ and the symbol $(')$ means derivative wrt the conformal time η. Latin indices run from 1 to 3. The effective pressure p_{eff} is the sum of an adiabatic component and the bulk viscous pressure (nonadiabatic). The VDF model is specified by $p = 0$ and a dissipationless fluid is recovered with $\xi = 0$.

In the conformal Newtonian gauge the line element for scalar perturbations of an isotropic and homogeneous, spatially flat universe is

$$ds^2 = a^2 (\eta) \left[-(1 + 2\phi) d\eta^2 + (1 - 2\psi) \delta_{ij} dx^i dx^j \right]. \tag{3.4}$$

The linear perturbations of the fluid 4-velocity are given by

$$u^0 = \frac{1}{a}(1 - \phi), \quad u_0 = -a(1 + \phi), \quad u^\gamma_{;\gamma} = \frac{3\mathcal{H}}{a} + \delta u^i_{,i} - \frac{3\mathcal{H}\phi}{a} - \frac{3\psi'}{a}. \tag{3.5}$$

For the linear perturbations of (3.2) we define the velocity scalar v, which is associated with the peculiar velocity by $\delta u^i_{,i} \equiv -kv/a$, where k is the comoving wavenumber. The perturbed components of (3.2) read

$$\delta T^0_0 = -\delta\rho, \tag{3.6}$$

$$\delta T^0_i = \frac{\rho}{a}(1 + w + w_{\text{v}})\delta u_i, \tag{3.7}$$

$$\delta T^i_j = \delta p \delta^i_j + \left[\xi(\frac{kv}{a} + \frac{3\mathcal{H}\phi}{a} + \frac{3\psi'}{a}) - \frac{3\mathcal{H}}{a}\delta\xi \right] \delta^i_j. \tag{3.8}$$

$\delta\xi$ denotes the perturbation of the coefficient of bulk viscosity. The adiabatic speed of sound $c^2_S \equiv (\partial p/\partial\rho)_S$. For dissipationless fluids, $c^2_S = p'/\rho'$ for the purposes of linear perturbation theory. For dissipative fluids in linear perturbation theory $c^2_S = (p'/\rho')_{\xi=0}$.

As we neglect anisotropic stresses in our model, the spatial off-diagonal Einstein equation implies $\phi = \psi$. At first order, the (0-0), (0-i) and the (i-i) components of the perturbed Einstein equation read ($\Delta \equiv \delta\rho/\rho$)

$$-k^2\psi - 3\mathcal{H}\psi' - 3\mathcal{H}^2\psi = \frac{3}{2}\mathcal{H}^2\Delta, \tag{3.9}$$

$$-k\left(\psi' + \mathcal{H}\psi\right) = \frac{3}{2}(1 + w + w_{\text{v}})\mathcal{H}^2 v, \tag{3.10}$$

$$\psi'' + 3\mathcal{H}\psi' - (w + w_{\text{v}})3\mathcal{H}^2\psi = \frac{3\mathcal{H}^2}{2}\left[\frac{\delta p}{\rho} - \frac{w_{\text{v}}}{3\mathcal{H}}\left(kv + 3\mathcal{H}\psi + 3\psi'\right) + w_{\text{v}}\frac{\delta\xi}{\xi}\right]. \tag{3.11}$$

The pressure perturbation $\delta p = c^2_S\delta\rho + \tau\delta S$, where δS denotes entropy perturbations and $\tau \equiv (\partial p/\partial S)_\rho$. Below we assume that pressure perturbations do not give rise to spatial fluctuations of the entropy to baryon ratio.

3.1 The integrated Sachs-Wolfe effect

The ISW effect is a net change in the energy of a CMB photon as it passes through evolving gravitational potential wells. It can be computed by

$$\left(\frac{\Delta T}{T}\right)_{\text{ISW}} = 2 \int_{\eta_r}^{\eta_0} d\eta \frac{\partial\psi}{\partial\eta} \left[(\eta_0 - \eta)\,\hat{\mathbf{n}}, \eta\right], \tag{3.12}$$

The integration is along the photon trajectory ($\hat{n}$) from η_r (conformal time at recombination) to η_0 (conformal time today).

Combining the equations (3.9) – (3.11) into a single expression for the gravitational potential, we end up with

$$\psi'' + \left(1 + c_S^2\right) 3\mathcal{H}\psi' + \left[\left(c_S^2 - w\right) 3\mathcal{H}^2 + c_S^2 k^2\right]\psi =$$
$$w_{\rm v}\left[\left[-\frac{1}{2} + \frac{k^2}{(1 + w + w_{\rm v})9\mathcal{H}^2}\right] 3\mathcal{H}\psi' + \left[\frac{3\mathcal{H}^2}{2} + \frac{k^2}{3(1 + w + w_{\rm v})}\right]\psi + \frac{3\mathcal{H}^2}{2}\Xi\right], \quad (3.13)$$

where $\Xi \equiv \delta\xi/\xi$ can be considered as the relative perturbation of the coefficient of bulk viscosity.

If we neglect the VDF contribution to the energy-momentum tensor, the right hand side of equation (3.13) vanishes and hence the resulting equation is the full evolution for the gravitational potential of an adiabatic fluid with an equation of state parameter $w = p/\rho$. The right hand side of (3.13) represents the influence of nonadiabaticity on ψ. For the VDF model, we set $c_S^2 = w = 0$ and use the appropriate functions $w_{\rm v}$ and $H_{\rm v}$. For the last term we need to know the functional form of ξ. If $\xi = \xi_0(\rho/\rho_0)^\nu$ its perturbation $\delta\xi = \nu\xi\Delta$ can be related to the potential ψ using equation (3.9).

3.2 Evolution of sub-horizon perturbations

In the radiation era pressure suppresses the growth of structures. However, cold dark matter, once kinetically decoupled from the plasma, starts to grow logarithmically on scales smaller than the Hubble horizon even during this epoch. Once the Universe becomes matter dominated ($z_{\rm eq} \sim 3000$) CDM can grow linearly in the scale factor. This scenario is called hierarchical structure formation as smallest structures form first and later on merge and grow to evolve into larger structures.

The unified dark matter models studied in this paper have a matter-like behavior in the past, but do not necessarily provide a successful structure formation scenario. In order to study scales which entered the horizon sufficiently long before matter-radiation equality, we make use of the covariant conservation of the energy-momentum tensor ($T^\mu_{\nu;\mu} = 0$). The first-order continuity equation reads

$$\Delta' - 3\mathcal{H}\Delta\left(w - c_S^2 + w_{\rm v}\right) - (1 + w + 2w_{\rm v})\left(kv + 3\psi'\right) - 3\mathcal{H}w_{\rm v}(\psi - \Xi) = 0, \quad (3.14)$$

and the Euler equation is

$$v' + \left[\mathcal{H}\left(1 - 3c_S^2 - 3w_{\rm v}\right) + \frac{w_{\rm v}'}{1 + w + w_{\rm v}} - \frac{w_{\rm v}k^2}{3\mathcal{H}\left(1 + w + w_{\rm v}\right)}\right]v -$$
$$\frac{w_{\rm v}k}{\mathcal{H}\left(1 + w + w_{\rm v}\right)}\psi' + \frac{k(1 + w)}{1 + w + w_{\rm v}}\psi + \frac{w_{\rm v}k}{1 + w + w_{\rm v}}\Xi + \frac{kc_S^2}{1 + w + w_{\rm v}}\Delta = 0. \quad (3.15)$$

For the adiabatic case there are many studies about the evolution of sub-horizon scales, even considering the possibility of energy other than matter or radiation [16] or modified theories of gravity [17]. However, the clustering properties of nonadiabatic CDM have not yet been considered in much detail.

For the VDF model ($w = c_S^2 = 0$), we can simplify equations (3.14) and (3.15) and take the subhorizon limit of the Poisson equation to obtain

$$\Delta' - 3\mathcal{H}w_{\mathrm{v}}\Delta = (1 + 2w_{\mathrm{v}})kv - 3\mathcal{H}w_{\mathrm{v}}\Xi \tag{3.16}$$

$$v' + \left[\mathcal{H}(1 - 3w_{\mathrm{v}}) + \frac{w_{\mathrm{v}}'}{1 + w_{\mathrm{v}}} - \frac{k^2 w_{\mathrm{v}}}{3\mathcal{H}(1 + w_{\mathrm{v}})}\right]v = -\frac{k\psi}{1 + w_{\mathrm{v}}} + \frac{kw_{\mathrm{v}}\psi'}{\mathcal{H}(1 + w_{\mathrm{v}})} - \frac{kw_{\mathrm{v}}\Xi}{1 + w_{\mathrm{v}}} \tag{3.17}$$

$$-k^2\psi = \frac{3}{2}\mathcal{H}^2\Delta \tag{3.18}$$

It is covenient to combine these equations to a single second-order differential equation for Δ and to use the scale factor a instead of conformal time. Hence, we obtain a Meszaros-like equation:

$$a^2\frac{d^2\Delta}{da^2} + \left[\frac{a}{H}\frac{dH}{da} + 3 + A(a) + B(a)k^2\right]a\frac{d\Delta}{da} + \left[+C(a) + D(a)k^2 - \frac{3}{2}\right]\Delta = P(a), \tag{3.19}$$

$$A(a) = -6w_{\mathrm{v}} + \frac{a}{1 + w_{\mathrm{v}}}\frac{dw_{\mathrm{v}}}{da} - \frac{2a}{1 + 2w_{\mathrm{v}}}\frac{dw_{\mathrm{v}}}{da} + \frac{3w_{\mathrm{v}}}{2(1 + w_{\mathrm{v}})}$$

$$B(a) = -\frac{w_{\mathrm{v}}}{3a^2 H^2(1 + w_{\mathrm{v}})}$$

$$C(a) = \frac{3w_{\mathrm{v}}}{2(1 + w_{\mathrm{v}})} - 3w_{\mathrm{v}} - 9w_{\mathrm{v}}^2 - \frac{3w_{\mathrm{v}}^2}{1 + w_{\mathrm{v}}}\left(1 + \frac{a}{H}\frac{dH}{da}\right) - 3a\left(\frac{1 + 2w_{\mathrm{v}}}{1 + w_{\mathrm{v}}}\right)\frac{dw_{\mathrm{v}}}{da} + \frac{6aw_{\mathrm{v}}}{1 + 2w_{\mathrm{v}}}\frac{dw_{\mathrm{v}}}{da}$$

$$D(a) = \frac{w_{\mathrm{v}}^2}{a^2 H^2(1 + w_{\mathrm{v}})}$$

$$P(a) = -3w_{\mathrm{v}}a\frac{d\Xi}{da} + 3w_{\mathrm{v}}\Xi\left[-\frac{1}{2} + \frac{9w_{\mathrm{v}}}{2} + \frac{-1 - 4w_{\mathrm{v}} + 2w_{\mathrm{v}}^2}{w_{\mathrm{v}}(1 + w_{\mathrm{v}})(1 + 2w_{\mathrm{v}})}a\frac{dw_{\mathrm{v}}}{da} - \frac{k^2(1 - w_{\mathrm{v}})}{3H^2 a^2(1 + w_{\mathrm{v}})}\right]$$

The function $P(a)$ contains all contributions from the perturbation of the coefficient of bulk viscosity $\delta\xi$. In the limit $w_{\mathrm{v}} = 0$ we obtain the standard equation for CDM perturbations with the solution $\Delta_{\mathrm{cdm}} \propto a$.

The above equations are solved numerically. However, in order to obtain some analytic predictions for Δ, note that in the sub-horizon limit $k \gg \mathcal{H}$ we find

$$a^2\frac{d^2\Delta}{da^2} + B(a)k^2 a\frac{d\Delta}{da} + D(a)k^2\Delta = -3w_{\mathrm{v}}a\frac{d\Xi}{da} - w_{\mathrm{v}}\Xi\frac{k^2(1 - w_{\mathrm{v}})}{H^2 a^2(1 + w_{\mathrm{v}})}. \tag{3.20}$$

If we also send w_{v} to -1, the k^2 terms dominate and the equation is dominated by the first derivative term, thus one can expect exponential damping.

4 Observational Constraints

4.1 Supernova and $H(z)$ data

We employ a statistical analysis using recent $H(z)$ [18] and the SN Ia constitution [19] data sets, in order to constrain the parameters of the background model.

The confidence contours for a set of parameters $\{\mathbf{p}\}$ are obtained from the probability distribution function (PDF)

$$P\left(\mathbf{p}\right) = \mathcal{B}e^{-\frac{\chi^2(\mathbf{p})}{2}},$$

where $\mathcal{B}$ is a normalization constant. For a given sample, lets say SN, χ^2 is defined by

$$\chi^2_{SN}(\mathbf{p}) = \sum_{\mathbf{i}} \frac{\left[\mu_{\mathbf{i}}^{\mathbf{th}}(\mathbf{p}) - \mu_{\mathbf{i}}^{\mathbf{obs}}(\mathbf{p})\right]^{\mathbf{2}}}{\sigma_{\mathbf{i}}^{\mathbf{2}}}. \tag{4.1}$$

The quantities μ_i^{th} and μ_i^{obs} are the theoretical and the observed values, of the distance moduli and σ_i denotes their error for each data point i. For the $H(z)$ sample we replace μ by H. Hence, for the joint analysis we use $\chi^2 = \chi^2_{SN} + \chi^2_H$.

Observational constraints on q_0 and ν are shown in Figure (1). It displays the 2σ and 3σ confidence levels with best fit at $(q_0, \nu) = (-0.95, -3.2)$ with $\chi^2_{Viscous} = 472.5$. The dashed-red lines are age constraints for which the Universe is 13Gyr and 15Gyr old. The parameters for which the transition to the accelerated epoch occurs at $z_{\mathrm{tr}} = 1$ and $z_{\mathrm{tr}} = 0.5$ are shown in the thin lines. We remark that these background results can be translated to the GCG model using the correspondences stablished in section 2. For the ΛCDM model (the horizontal line corresponding to $\nu = -0.5$) the best fit occurs at $q_0 = -0.57$ (vertical line) that means $\Omega_\Lambda = 0.71$. We obtain $\chi^2_{\Lambda CDM} = 472.9$. Thus the latter χ^2 is greater than for the viscous model. This occurs since the viscous model has an extra parameter. A model comparison by means of the Akaike information criterion, $AIC = \chi^2 + 2k$ with k being the number of free parameters [20], it becomes clear that both models are competitive with the ΛCDM model being slightly favoured ($|\Delta AIC| = 1.6$).

4.2 The integrated Sach-Wolfe effect from unified dark matter

The CMB spectrum of anisotropies has been a key test for dark energy candidates as well as for modified gravity theories. It has been observed that UDM models suffer from an amplification of the ISW signal [13]. In general, for the GCG, unless $\alpha = 0$, the acoustic peak to Sachs-Wolfe plateau ratio decreases for increasing $\alpha > 0$. A similar conclusion was obtained for the bulk viscous fluid in [13]. However, the dependence of these results on the free parameters of the UDM models is still not clear and we adress this question now.

We define a "quality" variable Q_m to measure the difference between the ISW signal for some model m and the ΛCDM model,

$$Q_m \equiv \frac{\left(\frac{\Delta T}{T}\right)^m_{\mathrm{ISW}}}{\left(\frac{\Delta T}{T}\right)^{\Lambda\mathrm{CDM}}_{\mathrm{ISW}}} - 1, \tag{4.2}$$

where positive (negative) values of Q stand for an enhanced (a reduced) ISW effect for the model m to ΛCDM. The signal $\left(\frac{\Delta T}{T}\right)^m_{\mathrm{ISW}}$ can be obtained from (3.12), once we have calculated the gravitational potential Ψ_m from (3.13). A similar definition of Q was considered in [21].
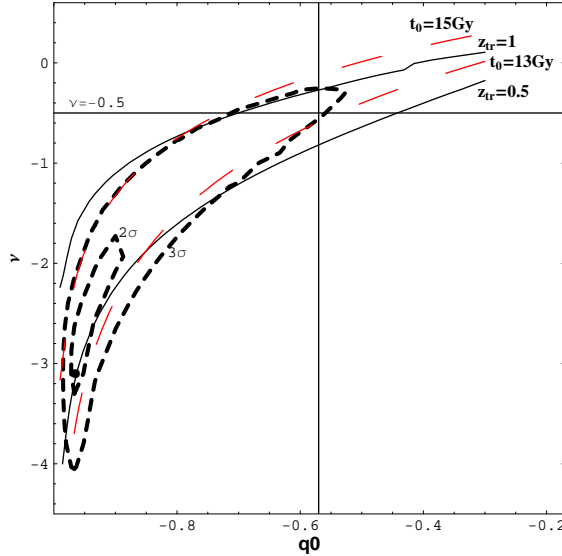
Figure 1. Observational constraints from SN1a and H(z) data on the parameters of the VDF model (q_0 and ν). The fat dot indicates the best-fit model. Short-dashed lines denote 2σ and 3σ contours. Long-dashed (red) lines indicate age constraints of 13 Gy and 15 Gy, respectively. Thin lines denote the redshift of the onset of accelerated cosmic expansion. The cosmic expansion history of a ΛCDM model is obtained for $\nu = -1/2$ (horizontal line) with its best fit at $q_0 = -0.57$ (vertical line).

The relevant modes for the ISW effect correspond to scales $k < 0.003(h/\text{Mpc})$, that is the approximate scale where the Sachs-Wolfe C_l plateau begins in the CMB temperature anisotropy angular power spectrum. We shall plot the contours $Q = 120\%, 80\%, 40\%$ and 0% in parameter space and compare them to the background constraints obtained above. With this strategy we verify whether it is possible to conciliate the ISW effect contours close to $Q = 0\%$ (i.e. close to the ΛCDM model) with the "allowed" background model parameters.

In order to estimate Q, we adopt a fiducial spatially flat ΛCDM model with parameters $H_0 = 72$ km/s/Mpc and $\Omega_{m0} = 0.266$, as suggested by WMAP-7.

One can ask if the current measurements of the ISW effect are able to discriminate between different models. In other words, are the values $Q = 40\%$ and 80% or even $Q = 120\%$ acceptable? To answer this question we consider current and future estimations of the error bars of the CMB temperature and galaxy cross-correlation function C_{gT}, that is currently used to measure the ISW effect [22]. Since the ISW effect is hard to measure one can currently discard only the models with $Q > 100\%$ (at 95%C.L.), corresponding to $2\delta C_{gT}/C_{gT} \geq 1$. Radio surveys in the near future will reduce the error up to a factor of 5 and thus should be able to improve the limit to the $Q = 20\%$ level (see figure 9 of [23]).

4.2.1 A model for $\xi(\rho)$ and its adiabatic counterpart

With the ansatz $\xi(\rho) = \xi_0(\rho/\rho_0)^\nu$ the quantity Ξ becomes

$$\Xi = \frac{2\nu}{3\mathcal{H}^2} \left(-k^2\psi - 3\mathcal{H}\psi' - 3\mathcal{H}^2\psi \right). \tag{4.3}$$

The evolution equation for the gravitational potential is obtained by combining (4.3) and (3.13). For the bulk viscous model ($c_s^2 = 0$) we solve it numerically and calculate Q_v

(see (4.2)) for various choices of the background parameters. The results are shown in figure (2). $Q = 0\%$ and even $Q = 40\%$ are in stark disagreement with the background contours (short-dashed lines) which are compatible with the constraints obtained in [24]. In additition, long-dashed lines display the age of the universe with 11, 13 and 15 Gyrs. The best-fit model, symbol • in Figure (2), corresponds to $Q_v = 120\%$.
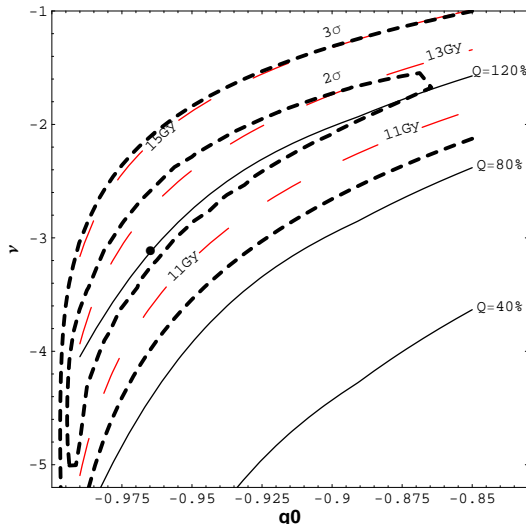

Figure 2. Additional CMB temperature fluctuations from the integrated Sachs-Wolfe effect are estimated by Q, see (4.2). Solid lines represent contours of constant Q_v are shown in together with the 2σ and 3σ contours and the age constraints of figure 1. VDF models with acceptable expansion history lead to at least a doubling of the ISW contributionwith respect to the WMAP 7yr best-fit ΛCDM model.

For the GCG model we compute equation (3.13) with $w_v = 0$. Also we write $\mathcal{H}$ as a function of A and α and for the adiabatic speed of sound we find

$$c_{s\,gc}^2 = -\alpha w_{gc} = \frac{\alpha A}{A + (1 - A)a^{-3(1+\alpha)}}. \tag{4.4}$$

We observe, see figure (3), a small improvement, as the best fit model is close to the $Q_{gc} = 80\%$ line. However, both cases are discarded by the CMB data and this result agrees with [12–14].

In section 3 the perturbation of the bulk viscous coefficient ($\delta\xi$) has been considered as a free function with its effects gathered by Ξ. Of course, a full perturbative analysis of the bulk viscous fluid should include this term. Let us for a moment take the freedom to treat Ξ as a free function of time neglecting the form imposed by (4.3). For the case $\Xi = cte = 0$ we observe that it is possible to conciliate the background constraints with the non-amplified ISW effect line ($Q_v = 0$) as shown in figure 4. We remark that the background dynamics is exactly the same as before and the nonadiabatic contributions, except for the term Ξ, are still active on the r.h.s. of (3.13). The analysis shown in figure 4 reveals that $\Xi \neq 0$ is the source of the amplified ISW effect which has plagued the VDF model. For $\zeta \propto \rho^\nu$, we cannot regard $\Xi = 0$ as a solution to the problem, since $\Xi = 0$ occurs only if $\nu = 0$ or $\Delta = 0$. We know that there are density fluctuations in the Universe, thus $\Delta \neq 0$. On the other hand,
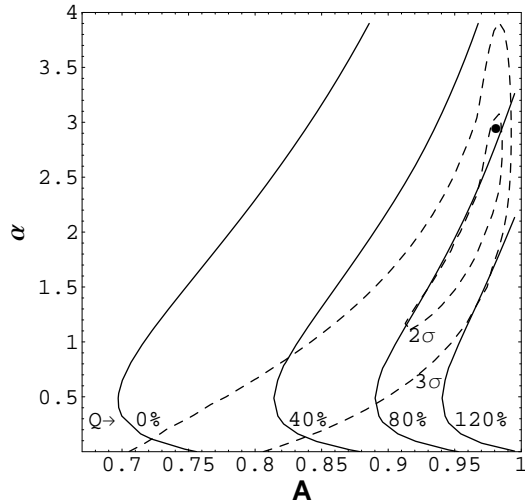
Figure 3. As figure 3, but now for the GCG model. The free parameters of the GCG model are A and α, as defined in the text. Dashed lines represent the 2σ and 3σ contours of the fit to SN1a and $H(z)$ data, with best-fit denoted by the fat dot. From left to right, the solid lines are contours of constant ISW contribution $Q_{\mathrm{gc}} = 0\%, +40\%, +80\%$ and $+120\%$. For the GCG the ISW effect is slightly less pronounced compared to the VDF models.

assuming $\nu = 0$ leads to very different background dynamics, which we study below as a particular configuration of the VDF model.
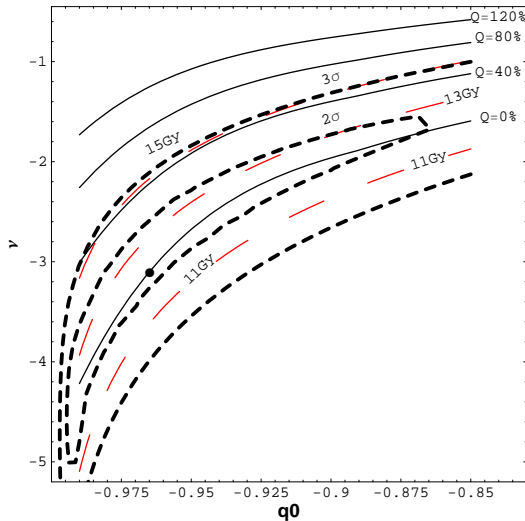
Figure 4. As figure 2, but now the perturbation of the coefficient of bulk viscosity is arbitrarily set to zero, $\delta\xi = 0$. ¿From top to botton the solid lines are the corresponding $Q_{\mathrm{v}} = +120\%, +80\%, +40\%$ and 0% contours. Long-dashed (red) lines display the age of the universe with 11, 13 and 15 Gy. Now, VDF models fit the background and do not show an enhanced ISW effect. However, there is no physical motivation to put $\delta\xi = 0$ in the context of VDF models, unless $\nu = 0$.

We have also verified that extremely large negative (positive) values for $\nu(\alpha)$ do not

produce a large amplification in the ISW effect. Concerning the GCG, this limit of the parameter α had been found before in [25] but the correspondence with ν had not yet been established. Large values for the parameter ν also agree with the analysis using the matter power spectrum [10]. This range for the parameter $\nu(\alpha)$ implies a step-transition of the background evolution from a CDM phase to a deSitter one as discussed in [26].

4.2.2 A constant coefficient of bulk viscosity

The previous considerations suggest to study the case of a constant coefficient of bulk viscosity ($\nu = 0$) in more detail. Now, the VDF has only q_0 as free parameter. At perturbative level there are no contributions from Ξ but the rhs of (3.13) is non-vanishing. Figure 5 shows the PDF for q_0 with the values $Q_{\rm v} = 120\%, 80\%, 40\%, 0\%$ and constraints from the age of the universe. The line $Q_{\rm v} = 0\%$ is within the 2σ region, but leads to a Universe younger than 13 Gyrs. In order to satistfy the age constraints $Q > 30\%$, which can be tested in the near future [23].
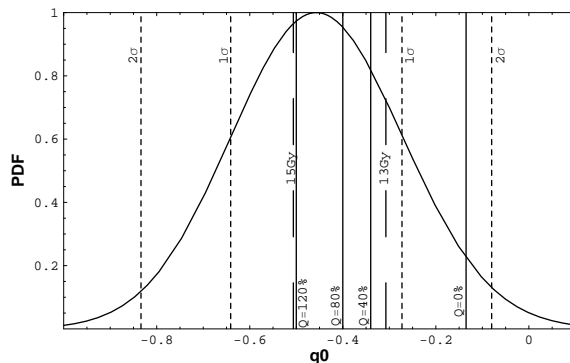

Figure 5. PDF for the case $\nu = 0$ with best fit at $q_0 = -0.46$. The short-dashed lines denote the 1σ and 2σ regions. The age constraints ($13Gy$ and $15Gy$) are shown by long-dashed lines. Solid lines represent, from left to right, $Q_{\rm v} = 120\%, 80\%, 40\%$ and 0%. The regions of a small enhancement of the ISW effect is in conflict with the age of the Universe.

4.2.3 Mimicking the ΛCDM background evolution

For $\nu = -0.5(\alpha = 0)$ the VDF (GCG) and the ΛCDM models have exactly the same background evolution. Hence, the ISW contribution from nonadiabatic perturbations can be quantified. Note that identical background solutions can be achieved by three different models: i)the ΛCDM scenario, ii) a two-fluid model consisting of pressureless, dissipationless matter and a dissipationless fluid with EoS $p = -\rho$, iii) the VDF(GCG) with $\nu = -0.5(\alpha = 0)$ which is also equivalent to a fluid with a negative constant pressure. On the other hand, these models have distinct perturbative dynamics, namely: i) there are no perturbations from Λ, ii) could have nontrivial but adiabatic perturbations and iii) has nontrivial and non-adiabatic perturbations. The GCG is an example for ii).

The result for the VDF with $\nu = -0.5$ is shown in the left panel in Figure 6. The nonadiabatic contributions of the VDF are responsible for putting the $Q_{\rm v} = 0\%$ line outside 3σ CL. However, if we neglect the contribution from $\delta\xi$, the $Q_{\rm v} = 0$ line is within the 1σ CL, right panel in Figure 6.

Concerning the GCG with $\alpha = 0$, the PDF for A parameter is shown in Figure 7. This particular case behaves very similar to the ΛCDM and our result agrees with [12].
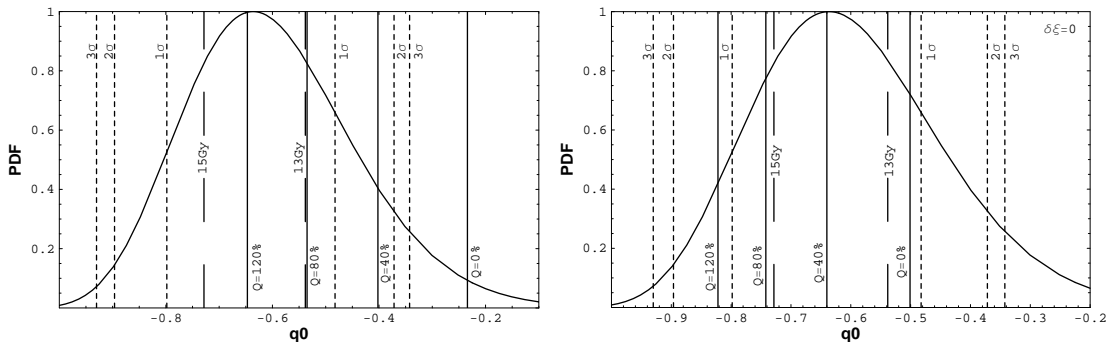

Figure 6. PDFs for the VDF with $\nu = -0.5$. The best fit occurs at $q0 = -0.64$. Left panel shows the result considering the full evolution while in the right panel the pertubation Ξ was neglected. The age constraints (13 Gy and 15 Gy) are shown as long-dashed lines. Solid lines represent, from left to right, $Q_{\mathrm{v}} = 120\%, 80\%, 40\%$ and 0%.
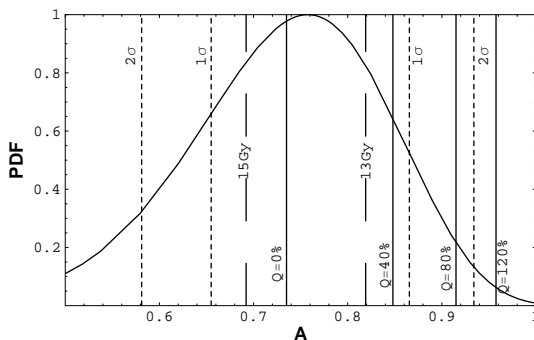

Figure 7. PDF for the GCG with $\alpha = 0$ and best fit at $A = 0.76$. The age constraints (13 Gy and 15 Gy) are shown as long-dashed lines. Solid lines represent, from left(right) to right(left), $Q_{\mathrm{gc}} = 120\%, 80\%, 40\%$ and 0%. This GCG model does not suffer from an ISW overproduction problem.

To summarize the observational constraints of sections 4.1 and 4.2, we have seen that generic VDF models that are excellent fits to SNIa and H(z) data sets, give rise to a large ISW contribution to the CMB temperature angular power spectrum and are thus excluded.

4.3   Structure formation on small scales

In the standard CDM structure formation scenario small-scale perturbations start to grow $\propto a$ when the universe becomes matter dominated, at a redshift z_{eq}. Before z_{eq}, even if the wavelength of the perturbation is larger than the Jeans length rapid expansion prevents the growth of structures. Hence, before we can study the process of strucutre formation for the VDF it is essential to establish the time at which the universe becomes VDF dominated and we thus include the radiation fluid in our analysis. With the inclusion of radiation the dynamics of the GCG remains the same. However, since the expansion rate becomes

$H = [\frac{8\pi G}{3}(\rho_v + \rho_r)]^{1/2}$ the background dynamics of the VDF is severely changed at early times. The fractional density for the VDF is given by the numerical solution of

$$a\frac{d\Omega_v}{da} + 3\Omega_v - \tilde{\xi}\Omega_v^\nu\left(\Omega_v + \frac{\Omega_{r0}}{a^4}\right)^{1/2} = 0, \tag{4.5}$$

where $\tilde{\xi} = 9H_0\xi_0\rho_c^{\nu-1}$, ρ_c is the critical density and $\Omega_{r0} = 8.475 \times 10^{-5}$. The new model parameter $\tilde{\xi}$ is related to the deceleration parameter q_0 approximately by

$$q_0 = \frac{1}{2}\left(1 + \frac{-9H_0\xi_0\rho_{v0}^\nu + \rho_{r0}}{\rho_{v0} + \rho_{r0}}\right) \approx \frac{1}{2}(1 - \tilde{\xi}). \tag{4.6}$$

The fiducial ΛCDM model adopted in section 3 has the matter-radiation equality occuring at $z_{eq} = 3137$. For a VDF plus radiation the equality is a function of the model parameters and will be denoted by z_{eq}^*. As shown in figure 8 for parameters values within 2σ CL, $z_{eq}^* > z_{eq}$. Hence, sub-horizon VDF fluid perturbations start to grow before typical CDM perturbations.
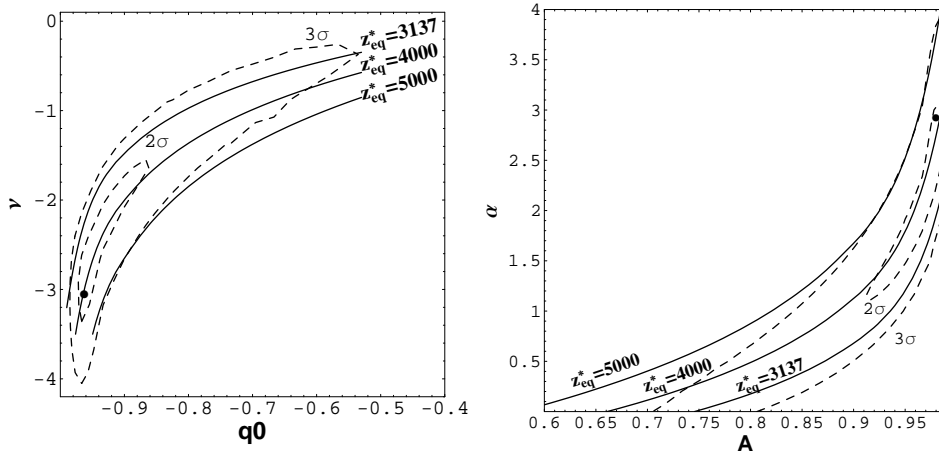

Figure 8. Redshift of matter-radiation equality for the VDF (left) and GCG (right). Countours of constant z_{eq}^* (see text) are shown in the model parameter space of the VDF (left) and GCG (right). Dashed lines denote the constraints from SN and H(z) data as presented in figures 1 and 3, respectively.

We solve equation (3.19) with intial conditions $\Delta_v(z_{eq*}) = 1$ and $\frac{d\Delta_v}{da}(z_{eq*}) = 1$ and compare with the CDM evolution $\Delta_{cdm} \propto a$ with the same initial conditions, however calculated at z_{eq}, $\Delta_{cdm}(z_{eq*}) = 1$ and $\frac{d\Delta_{cdm}}{da}(z_{eq*}) = 1$. The Hubble rate and equation of state function in (3.19) become

$$\left(\frac{H_v}{H_0}\right)^2 = \Omega_v + \Omega_{r0}a^{-4} \qquad w_v = -\frac{1-2q_0}{3}(\Omega_v + \Omega_{r0}a^{-4})^{1/2}\Omega_v^\nu, \tag{4.7}$$

with Ω_v being determined from (4.5).

We consider modes which give rise to cluster (subgalactic) size structures $k \sim 0.2\text{Mpc}^{-1}$ ($k = 10^6\text{Mpc}^{-1}$). We assume that for these modes the nonadiabatic Meszaros equation is valid up to the onset of non-linear evolution at $z_{nl} = 3(60 \pm 20)$ [27]. Soon after z_{nl}, a large fraction of the matter collapses into gravitationally bound objects. Nonlinear effects lead to

a further modification of the final (at $z = 0$) power spectrum. The study of them is beyond the scope of this work. Figure (9) shows the growth of perturbations, considering the best fit model obtained above, for $k = 0.2 – 0.3 \mathrm{Mpc}^{-1}$ ($k = 10^6 \mathrm{Mpc}^{-1}$) in left (right) panel. Also the CDM growth is shown as short-dashed line. If we consider the full evolution of equation (3.19) including the term Ξ (botton lines indicated by $\delta\xi \neq 0$) we observe a large growth suppression after a redshift $z \sim 6 (a \sim 0.14)$ for $k \sim 0.2 \mathrm{Mpc}^{-1}$ and $z \sim 200 (a \sim 0.005)$ for $k = 10^6 \mathrm{Mpc}^{-1}$. Indeed, the dominant contribution in the terms proportional to $k^2 \Delta$ and $k^2 \Delta'$ comes from Ξ and, consequently, at late times the density contrast Δ will decay rapidly. On the other hand, similarly to the ISW effect results, the perturbative dynamics is well behaved if $\delta\xi = 0$ (upper lines).

The GCG perturbations do not suffer any kind of suppression and will behave exactly like the CDM ones since it obeys the standard adiabatic growth equation, $w_v = 0$ in (3.19), with solution $\Delta_{\mathrm{gc}} \propto a$. At the same time, for any GCG configuration the transition to the accelerated expansion phase occurs after z_{nl} and the growth of perturbations is not suppressed by this effect.
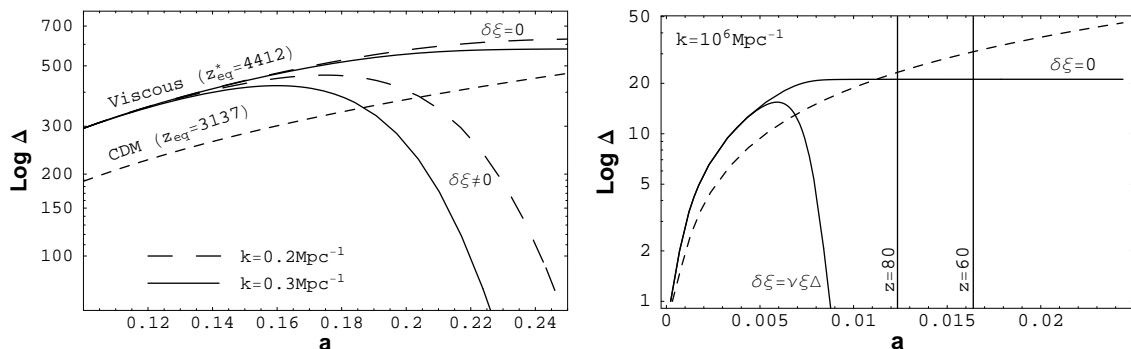

Figure 9. Left panel: Growth of sub-horizon perturbations in CDM (short-dashed) in the ΛCDM model and of the VDF for $k = 0.2 \mathrm{Mpc}^{-1}$ (long-dashed) and $k = 0.3 \mathrm{Mpc}^{-1}$ (solid). The upper lines for the viscous fluid have $\delta\xi = 0$, while the bottom ones have $\delta\xi = \nu\xi\Delta$. Right panel: The same for $k = 10^6 \mathrm{Mpc}^{-1}$. Generic VDF models supress structures on subgalactic scales exponentially.

5   Conclusions

The main idea behind the unification scenario is to reduce the dark sector to one component instead of dark energy and dark matter. This component should, at cosmological scales, reproduce both the structure formation process and the current accelerated expansion of the universe. The former condition seems to be the main challenge for such models.

We have compared the ISW signal of UDM models with the ΛCDM prediction. Figures (2) and (3) are in agreement with previous results, where the background-prefered model parameters of the VDF and the GCG imply an unacceptably large amplification of the ISW effect. In fact, we confirm and quantify the findings of [13] for a wide range of parameters. Although models with $\nu = 0$ cannot be ruled out by current data, they nevertheless show a significant amplification of the ISW effect that will be detectable in the future.

This tight constraints can be seen as an evidence that either bulk viscous effects do not play a role in the cosmic dynamics or that the phenomenological ansatz $\xi \sim \rho^\nu$ is not

appropriate. Since the intensive thermodynamic variables are functions of the extensive ones, a possible alternative is to describe the bulk viscous pressure in terms of energy density and entropy, i.e. $p = p(\rho, S)$ and $\xi = \xi(\rho, S)$. This could imply a well behaved perturbative dynamics and alleviate the *ISW problem* of such fluids. Recently a microscopic model for the cosmic bulk viscosity has been introduced as a dark energy candidate in [28]. This "dark goo" model shows good results when compared with the matter and CMB power spectrum. It could be interesting to extend this model to the context of unified dark matter where an estimation of the mass of the dark particle can be achieved. An important lesson from "dark goo is that more realistic viscosity coefficients show a complicated dependence on the energy density and cannot be written as $\zeta \propto \rho^\nu$.

On the other hand, we note that bulk viscous pressure represents a small negative correction to the positive equilibrium pressure. Here we have admitted the viscous pressure to be the dominating part of the pressure. This is clearly beyond the established range of validity of conventional non-equilibrium thermodynamics and non-standard interactions are required to support such an approach [29]. Hence, viscous cosmologies based on the Israel-Stewart theories [30] can also be considered. Recently, a qualitative analysis of such causal transport theory has been performed in [31].

We have studied the evolution of sub-horizon scales during the matter dominated epoch. In the standard CDM model the linear growth of small-scale perturbations gives rise to dark halos hosting galaxies. Concerning the unified scenario, we find a modification of the redshift of the matter-radiation equality. As shown in figure 8 the prefered parameter values for the UDM models are compatible with $z^*_{\rm eq} > z_{\rm eq}$. Hence, UDM perturbations start to grow earlier than CDM perturbations. The GCG perturbations follow the CDM growth $\Delta_{\rm gc} \propto a$ until z_{nl} and consequently, only the amplitude of the perturbations will be different. On the other hand, the VDF perturbations grow in a different way following a nonadiabatic Meszaros-like equation derived in section 3. In general, the evolution of Δ is scale-dependent and deviates significantly from ΛCDM. The most important effect at late times is the dominance of nonadiabatic contributions causing Δ to decay rapidly.

Despite the different evolution of viscous-matter perturbations and standard CDM perturbations on subhorizon scales, the *ad hoc* assumption $\delta\xi = 0$ can alleviate the Δ growth suppression. Since VDF perturbations start to grow before $z_{\rm eq}$, their amplitudes are of similar size as in the ΛCDM case. In other words, the growth before $z_{\rm nl}$ offsets the late time growth suppression. But this assumption is not an acceptable solution and unless other effects like shear viscosity or a very different ansatz for ξ would lead to qualitatively different results, the VDF models are ruled out. This can be interpreted as a complementary probe that viscous cosmologies based on the Eckart formalism (with $\xi \propto \rho^\nu$) are strongly challenged as potential contenders for a general relativity-based description of the cosmic medium.

The inclusion of a baryonic component in the system provides a more realistic model when compared with the one-fluid approximation adopted here. In this case, the background dynamics of the GCG fluid remains the same while the VDF will behave differently. However, as baryons represent a small fraction of the cosmic energy budget we do not expect a significant influence on the evolution of the unified dark sector.

To conclude, the dissipative UDM models considered in this work have severe problems to describe the observed cosmic structure on largest (enhanced ISW effect) and on smallest scales (overdamping due to dissipation).

Acknowledgments

References

[1] A. Yu. Kamenshchik, U. Moschella and V. Pasquier, Phys.Lett. B511 (2001) 265; J.C. Fabris, S.V.B. Gonçalves and P.E. de Souza, Gen. Rel. Grav. 34 (2002) 53 ; M. C. Bento, O. Bertolami and A. A. Sen, Phys. Rev. D66 (2002) 043507; N. Bilic, G. P. Tupper, and R. D. Viollier, Phys. Lett. B535 (2002) 17; N. Bilic, R. J. Lindebaum, G. P. Tupper, and R. D. Viollier, J. Cosmol. Astropart. Phys. 11 (2004) 008.

[2] Jackiw R, A particle field theorists lectures on supersymmetric, non-Abelian fluid mechanics and d-branes Preprint physics/0010042 (2000).

[3] J.C. Fabris, S.V.B. Gonçalves and R. de Sá Ribeiro, Gen. Rel. Grav. 38 (2006) 495; M. Szyd lowski and O. Hrycyna, Ann.Phys. 322 (2007) 2745; R. Colistete Jr., J.C. Fabris, J. Tossa and W. Zimdahl, Phys. Rev. D76 (2007) 103516.

[4] W. Zimdahl, D.J. Schwarz, A.B. Balakin, and D. Pavón, Phys. Rev. D 64 (2001) 063501.

[5] J. D. Barrow, Nucl. Phys. B **380** (1988) 743.

[6] S. del Campo and J. Villanueva, IJMPD 18 (2009) 2007; Puxum Wu and Hongwei Yu, ApJ, 658 (2007) 663; Jianbo Lu, Yuanxing Gui and Lixin Xu, Eur.Phys.J.C, 63 (2009) 349-354; Z.H. Zhu, Astron. Astrophys. 423 (2004)421; P.X. Wu and H.W. Yu, Phys. Lett. B 644 (2007)16.

[7] H. Sandvik, M. Tegmark, M. Zaldarriaga and I. Waga, Phys. Rev. D69 (2004) 123524.

[8] V. Gorini, A.Y. Kamenshchik, U. Moschella, O. F. Piatella, and A. A. Starobinsky, J. Cosmol. Astropart. Phys. 02 (2008) 016; J.C. Fabris, S.V.B. Gonçalves, H.E.S. Velten and W. Zimdahl, Phys. Rev. D 78 (2008) 103523; J.C. Fabris, H.E.S. Velten and W. Zimdahl, Phys. Rev. D 81 (2010) 087303.

[9] R. R. R. Reis, I. Waga, M. O. Calv?o and S. Joras, Phys. Rev. D **68** (2003) 061302; L. Amendola, I.Waga and F. Finelli, JCAP 0511 (2005) 009; Winfried Zimdahl and Julio C. Fabris, Class.Quant.Grav. 22 (2005) 4311-4324.

[10] W.S. Hipólito-Ricaldi, H.E.S. Velten and W. Zimdahl, JCAP 06 (2009) 016.

[11] W.S. Hipólito-Ricaldi, H.E.S. Velten and W. Zimdahl, Phys.Rev. D82 (2010) 063507 .

[12] L. Amendola, F. Finelli, C. Burigana and D. Carturan, JCAP 0307, (2003) 005; Chan-Gyung Park, Jai-chan Hwang, Jaehong Park and Hyerim Noh Phys.Rev.D81 (2010) 063532; Yuko Urakawa and Tsutomu Kobayashi JCAP 07(2010) 027.

[13] B. Li and J.D. Barrow, Phys. Rev. D79 (2009) 103521.

[14] Daniele Bertacca and Nicola Bartolo, JCAP 11 (2007) 026.

[15] C. Eckart, Phys. Rev. D58 (1940) 919.

[16] Seokcheon Lee and Kin-Wang Ng, Phys. Lett. B688 (2010)1-3; Christian G. Boehmer and Gabriela Caldera-Cabral, arXiv:1008.2852; S. Dodelson, Modern Cosmology (Academic Press, San Diego, 2002); P. Meszaros, Astrophys. J. 238 (1980) 781;

[17] Antonio De Felice, Shinji Mukohyama, and Shinji Tsujikawa, Phys.Rev.D82 (2010) 023524; Shinji Tsujikawa, Phys.Rev.D76 (2007) 023514; Seokcheon Lee, Mod.Phys.Lett.A23 (2008) 1388-1396.

[18] Daniel Stern, Raul Jimenez, Licia Verde, Marc Kamionkowski and S. Adam Stanford, JCAP 008 (2010) 02.

[19] M. Hicken et al., Astrophys.J. 700 (2009) 1097.

[20] H. Akaike, IEEE Transactions on Automatic Control 19, 6 (1974) 716.

[21] J.B. Dent, S. Dutta and T.J. Weiler, Phys. Rev. D79 (2009) 023502.

[22] Tommaso Giannantonio et al., Phys.Rev. D74 (2006) 063520; Marilena LoVerde, Lam Hui and Enrique Gaztanaga, Phys.Rev. D75 (2007) 043519.

[23] Alvise Raccanelli et al., arXiv:1108.0930.

[24] R. Colistete Jr., J. C. Fabris and S. V. B. Gonçalves, Int. J. Mod. Phys. D **14** (2005) 775; R. Colistete Jr. and J. C. Fabris, Class. Quant. Grav **22** (2005) 2813.

[25] Oliver Piattella, JCAP 1003 (2010) 012.

[26] Oliver F. Piattella, Daniele Bertacca, Marco Bruni and Davide Pietrobon, JCAP 01 (2010) 014.

[27] Anne M. Grenn, Stefan Hofmann and Dominik J. Schwarz, JCAP 08 (2005) 003.

[28] Jean-Sebastien Gagnon and Julien Lesgourgues, arXiv:1107.1503.

[29] A.B. Balakin, D. Pavón, D.J. Schwarz, and W. Zimdahl, NJP 5 (2003)85.

[30] W. Israel and J.M. Stewart, Proc. R. Soc. Lond. A365 (1979) 43; W. Israel and J.M. Stewart, Ann. Phys. 118 (1979) 341.

[31] Oliver F. Piattella. Júlio C. Fabris and Winfried Zimdahl, JCAP 1105 (2011) 029.